#### PHYSICAL REVIEW D 96, 015032 (2017)

# Vectorlike leptons: Muon g-2 anomaly, lepton flavor violation, Higgs boson decays, and lepton nonuniversality

Zijie Poh\* and Stuart Raby†

Department of Physics, The Ohio State University, 191 W. Woodruff Avenue, Columbus Ohio 43210, USA (Received 22 May 2017; published 26 July 2017)

In this paper, we consider the Standard Model (SM) with one family of vectorlike (VL) leptons, which couple to all three families of the SM leptons. We study the constraints on this model coming from the heavy-charged lepton mass bound, electroweak precision data, the muon anomalous magnetic moment, lepton flavor violation, Higgs boson decay constraints, and a recently measured lepton nonuniversality observable,  $R_{K^{*0}}$ , along with  $R_K$ . We find that the strongest constraints are coming from the muon g-2,  $R_{\mu\mu} = \Gamma(h \to \mu\mu)/\Gamma(h \to \mu\mu)_{\rm SM}$ ,  $R_{\gamma\gamma}$  and BR( $\mu \to e\gamma$ ). Although VL leptons couple to all three families of the SM leptons, the ratio of electron-VL to muon-VL coupling is constrained to be  $\langle \lambda_e/\lambda_\mu \rangle \lesssim 10^{-4}$ . We also find that this model cannot fit the lepton nonuniversality discrepancies.

## DOI: 10.1103/PhysRevD.96.015032

#### I. INTRODUCTION

The Standard Model (SM) is a highly successful theory in predicting and fitting many experimental measurements with few exceptions. One of the discrepancies between the SM prediction and experimental measurement that has been known for a long time, is the muon anomalous magnetic moment. The experimentally measured muon anomalous magnetic moment and the SM prediction are given by [1]

$$a_{\mu}^{\text{exp}} = 11659209.1(5.4)(3.3) \times 10^{-10},$$
  
 $a_{\mu}^{\text{SM}} = 11659180.3(0.1)(4.2)(2.6) \times 10^{-10}.$  (1)

The discrepancy between the experimental and theoretical values is [1]

$$\Delta a_{\mu} = a_{\mu}^{\text{exp}} - a_{\mu}^{\text{SM}} = 288(63)(49) \times 10^{-11}.$$
 (2)

A simple extension of the SM that is able to explain this discrepancy is the SM with one family of VL leptons. Dermíšek *et al.* showed that such a model with VL leptons coupling exclusively to the muon is sufficient to explain this discrepancy [2]. In a more natural theory, however, the VL leptons would couple to all three families of the SM leptons, which have been studied extensively in the literature [3–6]. Due to the lepton flavor violating nature of this model, the SM-VL couplings are known to be highly constrained.

In this paper, we try to provide a holistic point of view of the model in which the SM is extended by one family of VL leptons and the VL leptons have nonzero couplings to all three families of the SM leptons. We are interested in the constraints on this model coming from satisfying the heavy-charged lepton mass bound, electroweak precision data, the muon g-2, lepton flavor violation (LFV), Higgs boson decay constraints, and a recently measured lepton nonuniversality observable,  $R_{K^{*0}}$ , along with  $R_K$ . We find that this model cannot simultaneously satisfy electroweak precision measurements and the lepton nonuniversality discrepancies. As for the other observables, we find that the most constraining observables are the muon g-2,  $R_{\mu\mu} = \Gamma(h \to \mu\mu)/\Gamma(h \to \mu\mu)_{\rm SM}$ ,  $R_{\gamma\gamma}$  and  ${\rm BR}(\mu \to e\gamma)$ .

#### II. MODEL

The model that we study is the SM with one generation of VL leptons. The particles in the leptonic sector and their corresponding quantum numbers are given in Table I, and the leptonic sector Lagrangian is given by

$$\mathcal{L} \supset -\bar{\ell}_{Li} y_{ii}^e e_{Ri} H - \bar{\ell}_{Li} \lambda_i^E E_R H - \bar{L}_L \lambda_i^L e_{Ri} H$$
$$-\bar{L}_L \lambda E_R H - \bar{E}_L \bar{\lambda} L_R H^{\dagger} - M_L \bar{L}_L L_R$$
$$-M_E \bar{E}_L E_R + \text{H.c.}, \tag{3}$$

where i = 1, 2, 3 is the SM family index.

#### A. Lepton mass matrix

Without loss of generality, we assume that the SM lepton Yukawa matrix,  $y^e$ , is already diagonalized. Thus, the lepton mass matrix is

$$(\bar{e}_{Li} \ \bar{L}_L^- \ \bar{E}_L) \begin{pmatrix} y_{ii}^e v & 0 & \lambda_i^E v \\ \lambda_i^L v & M_L & \lambda v \\ 0 & \bar{\lambda} v & M_E \end{pmatrix} \begin{pmatrix} e_{Ri} \\ L_R^- \\ E_R \end{pmatrix} \equiv \bar{e}_{La} \mathcal{M} e_{Ra},$$

$$(4)$$

where a = 1, ..., 5. Let  $U_L$  and  $U_R$  be unitary matrices that diagonalize the charged lepton mass matrix,

poh.7@osu.edu raby.1@osu.edu

TABLE I. The quantum numbers of leptonic sector particles. i=1,2,3 is SM family index. The electric charge is given by  $Q=T_3+Y/2$  and the Higgs vacuum expectation value is 174 GeV. The fields h,  $\phi^+$ , and  $\phi^0$  are the physical Higgs boson and the would-be Nambu-Goldstone bosons, respectively, which give the  $W^{\pm}$  boson and Z boson mass.

	SM			VL	
	$\overline{\mathscr{C}_{Li} = \left(egin{array}{c}  u_{Li} \ e_{Li} \end{array} ight)}$	$e_{Ri}$	$H=\left(rac{\phi^+}{v+(h+i\phi^0)/\sqrt{2}} ight)$	$L_{L,R} = egin{pmatrix} L_{L,R}^0 \ L_{L,R}^- \end{pmatrix}$	$E_{L,R}$
$SU(2)_L$	2	1	2	2	1
$SU(2)_L$ $U(1)_Y$	-1	-2	1	-1	-2

$$U_L^{\dagger} \mathcal{M} U_R = \begin{pmatrix} M_{e_i} & 0 & 0 \\ 0 & M_{e4} & 0 \\ 0 & 0 & M_{e5} \end{pmatrix} \equiv \mathcal{M}^{\text{diag}}, \quad (5)$$

and the mass bases are

$$[\hat{e}_{L,R}]_a = [U_{L,R}^{\dagger}]_{a,a'} [e_{L,R}]_{a'}.$$
 (6)

In this model, neutrinos are assumed to only obtain a VL mass term,  $M_L$ .

#### **B.** Z-lepton couplings

The Z-lepton couplings are

$$\mathcal{L} \supset \frac{g}{c_W} Z_{\mu} [\bar{e}_{La} \gamma^{\mu} (T_a^3 + s_W^2) e_{La} + \bar{e}_{Ra} \gamma^{\mu} (T_a^3 + s_W^2) e_{Ra}], \quad (7)$$

where  $s_W = \sin \theta_W$ ,  $c_W = \cos \theta_W$  and  $T_a^3$  is the SU(2) generator where

$$T_a^3 e_{La} = -\frac{1}{2} \operatorname{diag}(1, 1, 1, 1, 0) e_{La} \equiv T_L^3 e_{La}$$
 (8)

$$T_a^3 e_{Ra} = -\frac{1}{2} \operatorname{diag}(0, 0, 0, 1, 0) e_{Ra} \equiv T_R^3 e_{Ra}.$$
 (9)

Since these matrices are not proportional to the identity matrix, when we rotate to the lepton mass basis, the *Z*-lepton couplings are not diagonal,

$$\mathcal{L} \supset Z_{\mu} [\bar{\hat{e}}_{La} \gamma^{\mu} g_{Lab}^{Z} \hat{e}_{Lb} + \bar{\hat{e}}_{Ra} \gamma^{\mu} g_{Rab}^{Z} \hat{e}_{Rb}], \qquad (10)$$

where  $g_{L,R}^Z=(g/c_W)[U_{L,R}^\dagger(T_{L,R}^3+s_W^2)U_{L,R}]$ . Hence, this model has LFV Z boson decays.

## C. W-lepton couplings

The W-lepton couplings are

$$\mathcal{L} \supset \frac{g}{\sqrt{2}} W_{\mu}^{+} [\bar{\nu}_{La} \gamma^{\mu} e_{La} + \bar{\nu}_{Ra} \gamma_{\mu} e_{Ra}] + \text{H.c.}, \quad (11)$$

where

$$\nu_{La} = \begin{pmatrix} \nu_{Li} \\ L_L^0 \\ 0 \end{pmatrix}, \quad \text{and} \quad \nu_{Ra} = \begin{pmatrix} 0_i \\ L_R^0 \\ 0 \end{pmatrix}. \tag{12}$$

Hence, in the charged lepton mass basis, we have

$$\mathcal{L} \supset W_{\mu}^{+} [\bar{\nu}_{La} \gamma^{\mu} g_{Lab}^{W} \hat{e}_{Lb} + \bar{\nu}_{Ra} \gamma_{\mu} g_{Rab}^{W} \hat{e}_{Rb}] + \text{H.c.}, \quad (13)$$

where  $g_L^W = (g/\sqrt{2}) \text{diag}(1, 1, 1, 1, 0) U_L$  and  $g_R^W = (g/\sqrt{2}) \times \text{diag}(0, 0, 0, 1, 0) U_R$ .

# D. Higgs-lepton couplings

The couplings between the physical Higgs boson and the leptons are

$$\mathcal{L} \supset -\frac{1}{\sqrt{2}} h \bar{e}_{La} Y^e_{ab} e_{Rb} + \text{H.c.}, \tag{14}$$

where

$$Y^{e} = \begin{pmatrix} y_{ii}^{e} & 0 & \lambda_{i}^{E} \\ \lambda_{i}^{L} & 0 & \lambda \\ 0 & \bar{\lambda} & 0 \end{pmatrix}. \tag{15}$$

In the mass basis, we have

$$\mathcal{L} \supset -\frac{1}{\sqrt{2}} h \bar{\hat{e}}_{La} \hat{Y}^e_{ab} \hat{e}_{Rb} + \text{H.c.}, \tag{16}$$

where

$$\hat{Y}^e = U_L^{\dagger} Y^e U_R. \tag{17}$$

This Yukawa matrix is nondiagonal because  $Y^e v = \mathcal{M} - \text{diag}(0, 0, 0, M_L, M_E)$ . Hence,

$$\hat{Y}^e = \mathcal{M}^{\text{diag}}/v - U_L^{\dagger} \text{diag}(0, 0, 0, M_L, M_E) U_R/v, \quad (18)$$

where the second term is nondiagonal.

## E. Lepton nonuniversality

To calculate the effect of this model on lepton nonuniversality, we consider the following Hamiltonian [7,8]

$$\mathcal{H}_{\text{eff}} = -\frac{4G_F}{\sqrt{2}} V_{tb} V_{ts}^* \frac{e^2}{16\pi^2} \sum_{j=9,10} C_j O_j, \qquad (19)$$

where

$$\mathcal{O}_9 = (\bar{s}_L \gamma^\mu b_L)(\bar{\hat{e}}_a \gamma_\mu \hat{e}_a), \tag{20}$$

$$\mathcal{O}_{10} = (\bar{s}_L \gamma^\mu b_L)(\bar{\hat{e}}_a \gamma_\mu \gamma_5 \hat{e}_a). \tag{21}$$

The new physics (NP) contribution to these two Wilson coefficients are coming from the box diagrams in Fig. 1 (see the appendix for calculation [9])

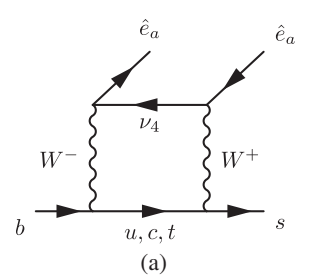
$$C_9^{\text{NP}} = -\frac{1}{s_W^2} \frac{1}{4} [U_1^+(x, y)g_1(x, y) + U_0^+(x, y)g_0(x, y)],$$

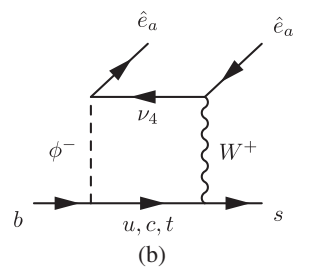
$$C_{10}^{\text{NP}} = \frac{1}{s_W^2} \frac{1}{4} [U_1^-(x, y)g_1(x, y) + U_0^-(x, y)g_0(x, y)], \qquad (22)$$

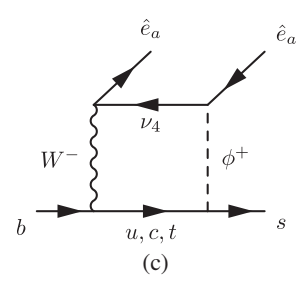
where  $x = M_t^2/M_W^2$ ,  $y = M_L^2/M_W^2$ ,

$$Y^{\nu_L} \equiv \begin{pmatrix} y_{ii}^e & 0 & \lambda_i^E \\ \lambda_i^L & 0 & \lambda \\ 0 & 0 & 0 \end{pmatrix}, \tag{23}$$

$$Y^{\nu_R \dagger} \equiv \begin{pmatrix} 0 & 0 & 0 \\ 0 & 0 & 0 \\ 0 & \bar{\lambda} & 0 \end{pmatrix}, \tag{24}$$







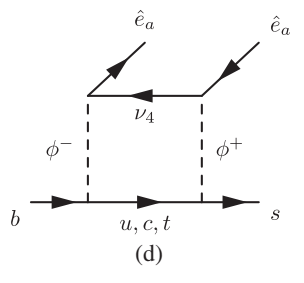


FIG. 1. Box diagrams contributing to  $b \rightarrow s\hat{e}_a\hat{e}_a$ .

$$g_1(x,y) = \frac{1}{x-y} \left[ \frac{x^2}{(x-1)^2} \log x - \frac{y^2}{(y-1)^2} \log y - \frac{1}{x-1} + \frac{1}{y-1} \right],$$
 (25)

$$g_0(x,y) = \frac{1}{x-y} \left[ \frac{x}{(x-1)^2} \log x - \frac{y}{(y-1)^2} \log y - \frac{1}{x-1} + \frac{1}{y-1} \right],$$
 (26)

and

$$U_{1}^{\pm}(x,y) = |[U_{L}]_{4a}|^{2} \pm |[U_{R}]_{4a}|^{2} + \frac{1}{4} \frac{v^{2}}{M_{L}^{2}} xy(|[Y^{\nu_{R}}U_{L}]_{4a}|^{2} \pm |[Y^{\nu_{L}}U_{R}]_{4a}|^{2}), \quad (27)$$

$$U_0^{\pm}(x,y) = -\frac{v}{M_L} xy([U_L]_{4a} [Y^{\nu_R*}U_L^*]_{4a} + [U_L^*]_{4a} [Y^{\nu_R}U_L]_{4a}$$

$$\pm [U_R]_{4a} [Y^{\nu_L*}U_R^*]_{4a} \pm [U_R^*]_{4a} [Y^{\nu_L}U_R]_{4a}). \quad (28)$$

#### III. PROCEDURE

The analysis of this paper is similar to that in [2]. A new feature of this paper is that VL leptons are not assumed to couple exclusively to muons. Instead, VL leptons couple to all three families of SM leptons, and we are interested in the constraints of the 10 model parameters: VL Masses,  $M_{L,E}$ ; VL-VL couplings,  $\lambda$ ,  $\bar{\lambda}$ ; and SM-VL couplings,  $\lambda_{e,\mu,\tau}^{L,E}$ .  $y_{e,\mu,\tau}$  are not free parameters because  $y_{e,\mu,\tau}$  are chosen such that  $m_{e,\mu,\tau}$  are the central values in Particle Data Group (PDG) [1]. We considered  $M_{L,E} \in (100, 1000)$  GeV and  $\lambda$ ,  $\bar{\lambda} \in (-1, 1)$ . As for the SM-VL couplings, we considered

$$\frac{\lambda_{e,\mu,\tau}^{L,E}v}{M_{L,E}} \in (-0.09, 0.09). \tag{29}$$

The ranges of the SM-VL couplings are chosen to satisfy the electroweak constraints.<sup>1</sup>

The constraints that we consider in this paper are from the heavy charged lepton mass bound, precision electroweak data, the muon g-2, LFV, Higgs decays, and lepton nonuniversality observables. See Table II for the complete list of observables. All of the experimental values, other than lepton nonuniversality observables, are taken from the PDG [1]. The experimental value for  $R_K$  is taken from Ref. [10], while  $R_{K^{*0}}$  is recently measured by LHCb [11].

<sup>&</sup>lt;sup>1</sup>With our upper limit on  $M_{L,E}=1000$  GeV, this implies an upper bound on the dimensionless couplings  $\lambda_{e,\mu,\tau}^{L,E}\lesssim 0.5$ .

TABLE II. List of observables.  $\Delta a_{\mu}$  is the discrepancy of the measured muon g-2 and the SM prediction.  $A_{e,\mu,\tau}$  is the electron, muon, and tau left-right asymmetry in Z decay.  $A_{FB}^{(0e),(0\mu),(0\tau)}$  is the electron, muon, and tau forward-backward asymmetry in Z decay.  $R_{\mu\mu} = \Gamma(h \to \mu\mu)/\Gamma(h \to \mu\mu)_{\rm SM}$  and similarly for  $R_{\tau\tau}$  and  $R_{\gamma\gamma}$ .  $R_K = \Gamma(B^+ \to K^+\mu\mu)/\Gamma(B^+ \to K^+ee)$  while  $R_{K^{*0}} = \Gamma(B^0 \to K^{*0}\mu\mu)/\Gamma(B^0 \to K^{*0}ee)$ . Lepton nonuniversality experimental values are take from LHCb measurements [10,11] while the other experimental values are taken from PDG [1].

Muon $g-2$	$\mu$	$\Delta a_{\mu}$
Heavy charged leptons	$e_4$	$M_{e4}^{r}$
	Z	$A_{e,\mu, au},A_{FB}^{(0e),(0\mu),(0 au)} \ \mathrm{BR}(Z o ee),\mathrm{BR}(Z o \mu\mu),\mathrm{BR}(Z o  au au)$
Electroweak precision	W	$BR(W \to e\nu_e)$ , $BR(W \to \mu\nu_\mu)$ , $BR(W \to \tau\nu_\tau)$
	$\mu$	$BR(\mu \to e \bar{\nu}_e \nu_\mu)$
	au	$BR(\tau \to e\bar{\nu}_e\nu_\tau), BR(\tau \to \mu\bar{\nu}_e\nu_\tau)$
	Z	$BR(Z \to e\mu), BR(Z \to e\tau), BR(Z \to \mu\tau)$
Lepton flavor violation	$\mu$	$BR(\mu \to e\gamma), BR(\mu \to 3e)$
Lepton havor violation	τ	BR $(\tau \to e\gamma)$ , BR $(\tau \to \mu\gamma)$ BR $(\tau \to 3e)$ , BR $(\tau \to 3\mu)$
Higgs	h	$R_{\mu\mu}, R_{\tau\tau}, R_{\gamma\gamma}, BR(h \to \mu\tau)$
Lepton nonuniversality	B meson	$R_K,\ R_{K^{*0}}$

The heavy charged lepton mass bound quoted by the PDG, M > 100.8 GeV, is from the LEP experiment. There are more recent bounds on the mass of VL leptons obtained from reinterpreting ATLAS and CMS experiments [12–15]. If the lightest VL lepton is predominantly  $E_{L,R}$ , then the bound is similar to the LEP bound. However, if the lightest VL lepton is predominantly  $L_{L,R}$ , then the bound can be more stringent. For example, Falkowski et al. showed that if the VL lepton decays only to e and  $\mu$ , then the bound is  $M_{e4} \gtrsim 450 \text{ GeV}$  [12]. On the other hand, Kumar et al. showed that if the VL lepton decays only to  $\tau$ , then the bound may only be  $M_{e4} \gtrsim 275 \text{ GeV}$  [15]. Due to the sampling method that we explain below, VL leptons in this model can either be predominantly  $E_{L,R}$  or  $L_{L,R}$ , depending on model parameters. In addition, VL leptons of this model can decay to all three SM leptons. Hence, reinterpretations of the ATLAS and CMS analyses are needed to obtain the bound on this model. To be conservative, we have decided to use the LEP bound in this paper while keeping in mind that more stringent bounds may exist.

All theoretical calculations are performed at leading order, that is, all observables other than  $\Delta a_{\mu}$ ,  $\mathrm{BR}(\ell \to \ell' \gamma)$ ,  $R_{\gamma \gamma}$ ,  $R_K$ ,  $R_{K^{*0}}$  are calculated at tree level. The effect of one-loop calculations are expected to be small. The theoretical calculation of the VL contribution to the muon g-2 is taken from Ref. [2]. The calculation for  $\mathrm{BR}(\ell \to \ell' \gamma)$  and  $R_{\gamma \gamma}$  are performed at one-loop [16,17]. Since all calculations are performed at leading order, we have included a 1% theoretical error when ensuring that the calculated observables satisfy the current experimental bounds. As for the lepton nonuniversality analysis, we have used flavio, a very versatile program that calculates b-physics observables written by Straub et al. [18]. To calculate the NP effects of the observables implemented in

flavio, one only has to specify the NP contribution to the Wilson coefficients.

In the analysis, we obtain scatter plots by sampling from the parameter space and checking to see if the sampled points satisfy the constraints mentioned above. To ensure that we cover all regions in this vast parameter space, we divide VL masses into four different regions:  $M_{L,E} \in$ [100, 150), [150, 250), [250, 500), [500, 1000) GeV, and the VL-VL couplings into two different regions<sup>2</sup>:  $|\lambda|, |\bar{\lambda}| \in [0, 0.75), [0.75, 1)$ . As for the muon-VL couplings, we considered  $|\lambda_{\mu}^{L,E}v/M_{L,E}| \in [0, 0.06), [0.06,$ 0.09). For each of these regions, we sampled 10,000 points satisfying the heavy charged lepton mass bound and the electroweak precision observables. The total number of simulated points is 2.56 millions points. The parameters  $M_{LE}$ ,  $\lambda$ ,  $\bar{\lambda}$ ,  $\lambda_{\mu}^{L,E}$  are sampled from a uniform distribution while  $|\lambda_{e,\tau}^{L,E} v/M_{L,E}| \in [10^{-10}, 0.09)$  are sampled from a loguniform distribution. The electron-VL and tau-VL couplings are sampled from a log-uniform distribution, because we expect these couplings to be highly constrained by LFV observables and we are interested in determining the degree of fine-tuning of these two parameters in order to be consistent with the flavor violation constraints.

# IV. RESULTS

In this section, we present the results of our numerical analysis. For all plots in this section, we have classified the simulated points into two groups. This classification is based on whether a point satisfies all observables listed in Table II other than the plotted observables and the lepton

<sup>&</sup>lt;sup>2</sup>These couplings can be positive or negative. The quoted ranges are the magnitude. Similarly for SM-VL couplings.

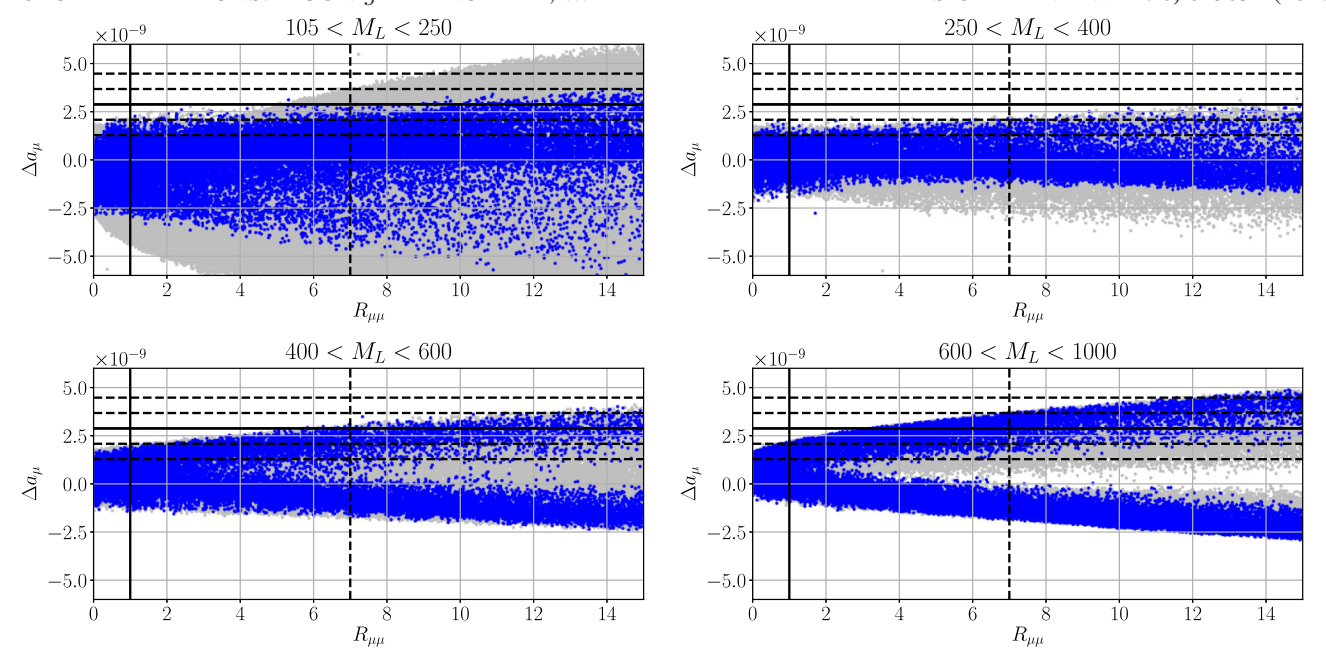


FIG. 2. Plots of the muon g-2 discrepancy,  $\Delta a_{\mu}$ , versus  $R_{\mu\mu} = \Gamma(h \to \mu\mu)/\Gamma(h \to \mu\mu)_{\rm SM}$ . The four plots have different ranges of  $M_L$ . The gray points are ruled out. The dashed lines show the  $1\sigma$  and  $2\sigma$  bounds of  $\Delta a_{\mu}$  and the upper bound of  $R_{\mu\mu}$ . The solid lines show the central value of  $\Delta a_{\mu}$  and  $R_{\mu\mu} = 1$ .

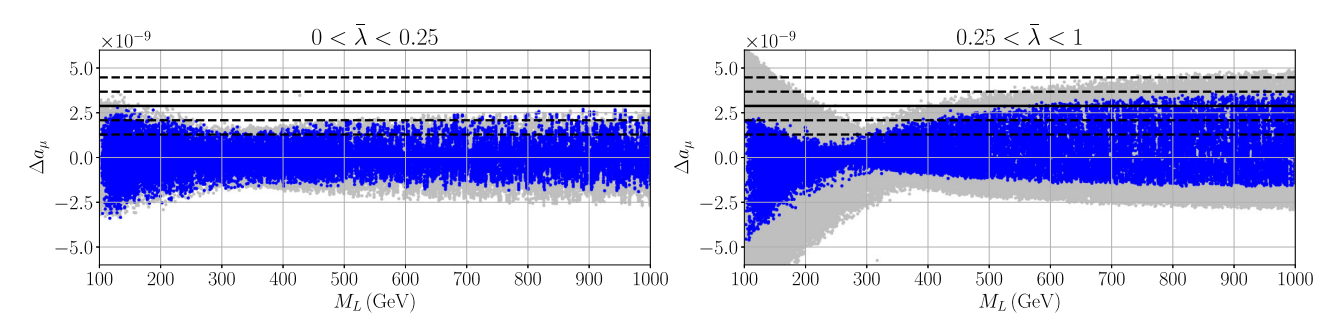


FIG. 3. Plots of  $\Delta a_{\mu}$  versus  $M_L$ . The two plots have different ranges of  $\bar{\lambda}$ . The gray points are ruled out. The dashed lines are the  $1\sigma$  and  $2\sigma$  bounds of  $\Delta a_{\mu}$  while the solid line is the central value of  $\Delta a_{\mu}$ .

nonuniversality observables. The lightly shaded points do not satisfy one or more of these observables, while the solid colored points satisfy all of these observables.

Figure 2 shows plots of  $\Delta a_{\mu}$  versus  $R_{\mu\mu}$ . The four plots have different ranges of  $M_L$ , which is a meaningful discriminator because the VL contribution to the muon g-2 from the W boson loop is due to the SU(2) doublet VL neutrinos,  $L_{L,R}^0$ , which have a mass  $M_L$  [2]. The dashed lines show the  $1\sigma$  and  $2\sigma$  bounds of  $\Delta a_{\mu}$ , and the upper bound of  $R_{\mu\mu}$ . The solid lines show the central value of  $\Delta a_{\mu}$  and  $R_{\mu\mu}=1.3$  From this figure, we see that this model can be ruled out in the future if future measurements of the muon g-2 and  $R_{\mu\mu}$  have much smaller uncertainties, and

 $R_{\mu\mu}$  is measured to be SM-like, while the muon g-2 is measured to have a similar central value.

Figure 2 also shows that the there are no points with 250 GeV <  $M_L$  < 400 GeV that fit the muon g-2 within  $1\sigma$ . This observation is further illustrated in Fig. 3, which shows plots of  $\Delta a_{\mu}$  versus  $M_L$ . The two plots have different ranges of  $\bar{\lambda}$ . This figure shows that for  $\bar{\lambda}$  < 0.25, this model requires either  $M_L$  < 250 GeV or  $M_L$  > 600 GeV to fit the muon g-2 within  $1\sigma$ . On the other hand, this model requires  $M_L$  > 400 GeV for  $\bar{\lambda}$  > 0.25. This plot also shows that the allowed parameter space for  $M_L \lesssim$  250 GeV can potentially be eliminated by the upcoming Fermilab E989

<sup>&</sup>lt;sup>3</sup>Notice that there is no measurement of  $R_{\mu\mu}$  yet. There is only an upper bound.

<sup>&</sup>lt;sup>4</sup>The bounds on parameter space obtained are not strict because the analysis is performed by random sampling from the vast parameter space. Our sampling method attempts to cover the whole parameter space, but there might still be regions that are missed by the sampling method.

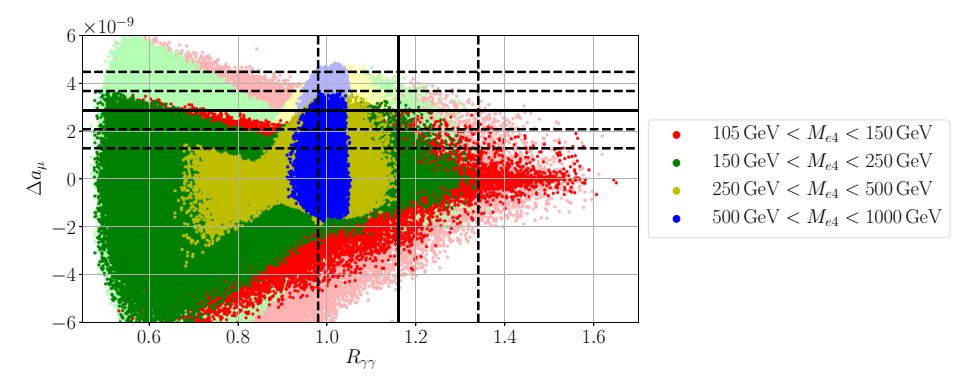


FIG. 4. Plot of  $\Delta a_{\mu}$  versus  $R_{\gamma\gamma}$ . The lightly shaded points are ruled out. The dashed lines show the  $1\sigma$  and  $2\sigma$  bounds of  $\Delta a_{\mu}$ , and the  $1\sigma$  bound of  $R_{\gamma\gamma}$ . The solid lines show the central value of  $\Delta a_{\mu}$  and that of  $R_{\gamma\gamma}$ .

experiment if the muon g-2 central value stays the same while the uncertainties decrease by a couple factors [19].

In general, as the VL masses increase, the new physics effects should approach zero. However, Fig. 3 seems to violate this fact. The muon g-2 does not approach zero as  $M_L$  increases because other parameters, such as  $M_E$ ,  $\bar{\lambda}$ , and  $\lambda_{\mu}^{L,E}$ , are not fixed. In fact, if all of the other parameters are fixed, then the muon g-2 approaches zero as  $M_L$  increases.

Figure 4 shows a plot of  $\Delta a_{\mu}$  versus  $R_{\gamma\gamma}$ . The points in this plot are separated into different colors based on  $M_{e4}$ . As expected, for heavier VL mass eigenstates,  $R_{\gamma\gamma}$  is clustered around one. This plot shows that  $M_{e4} > 500$  GeV is a more robust region than regions with smaller  $M_{e4}$  because a larger percentage of simulated points are within the experimental bounds. A very interesting scenario

will arise if the central value of  $R_{\gamma\gamma}$  stays and uncertainties in the measurement decrease as more data are collected. In this scenario, we will have the potential to place an upper bound on the mass of the lightest VL mass eigenstate because there are no points with  $M_{e4} > 500~{\rm GeV}$  and  $R_{\gamma\gamma} \gtrsim 1.1$ .

In Fig. 5, which shows plots of  $\Delta a_{\mu}$  versus  $R_{\gamma\gamma}$ , the points are separated into four different plots based on different values of

$$\|\lambda_{\mu}\| \equiv \sqrt{\left(\frac{\lambda_{\mu}^{L} v}{M_{L}}\right)^{2} + \left(\frac{\lambda_{\mu}^{E} v}{M_{E}}\right)^{2}}.$$
 (30)

 $\|\lambda_{\mu}\|$  is a meaningful variable because muon-VL couplings play a significant role in fitting  $\Delta a_{\mu}$ , and this variable captures the norm of the muon-VL coupling normalized by

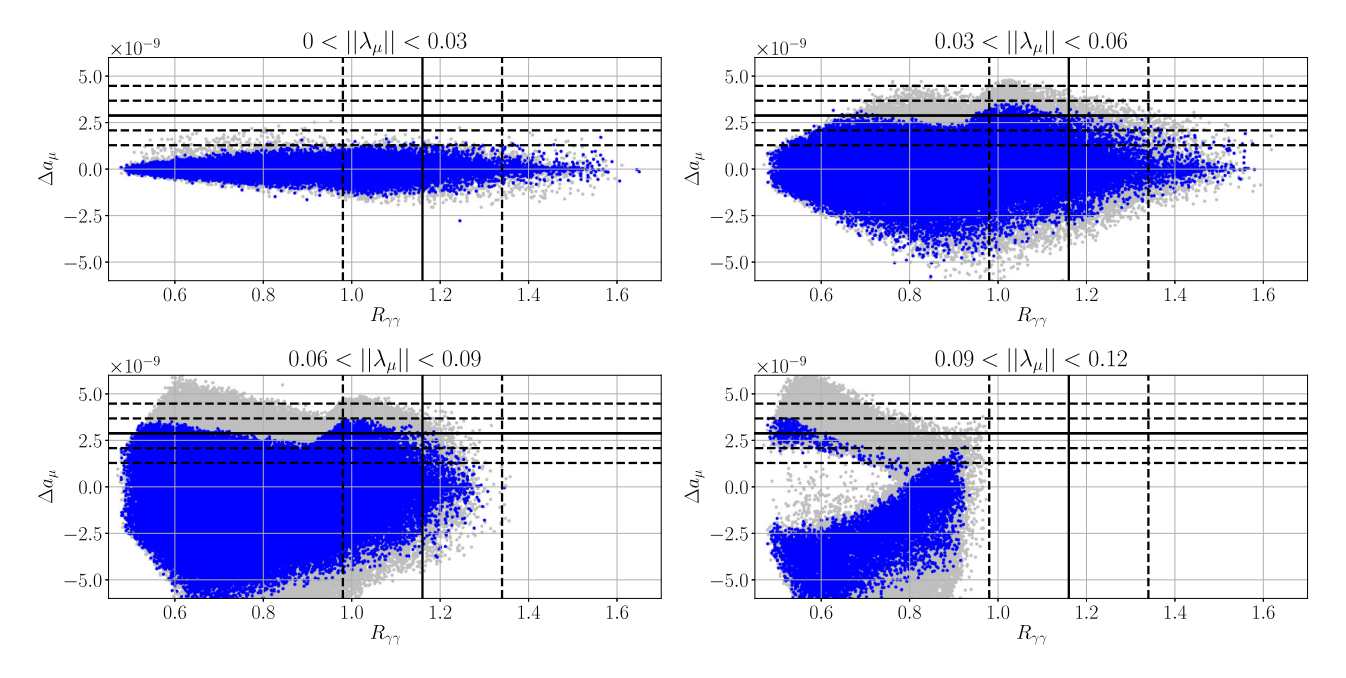


FIG. 5. Plots of  $\Delta a_{\mu}$  versus  $R_{\gamma\gamma}$ . The gray points are ruled out. The dashed lines show the  $1\sigma$  and  $2\sigma$  bounds of  $\Delta a_{\mu}$ , and the  $1\sigma$  bound of  $R_{\gamma\gamma}$ . The solid lines show the central value of  $\Delta a_{\mu}$  and that of  $R_{\gamma\gamma}$ . This model requires  $\|\lambda_{\mu}\| > 0.03$  to fit  $\Delta_{\mu}$  and  $\|\lambda_{\mu}\| < 0.09$  to fit  $R_{\gamma\gamma}$ .

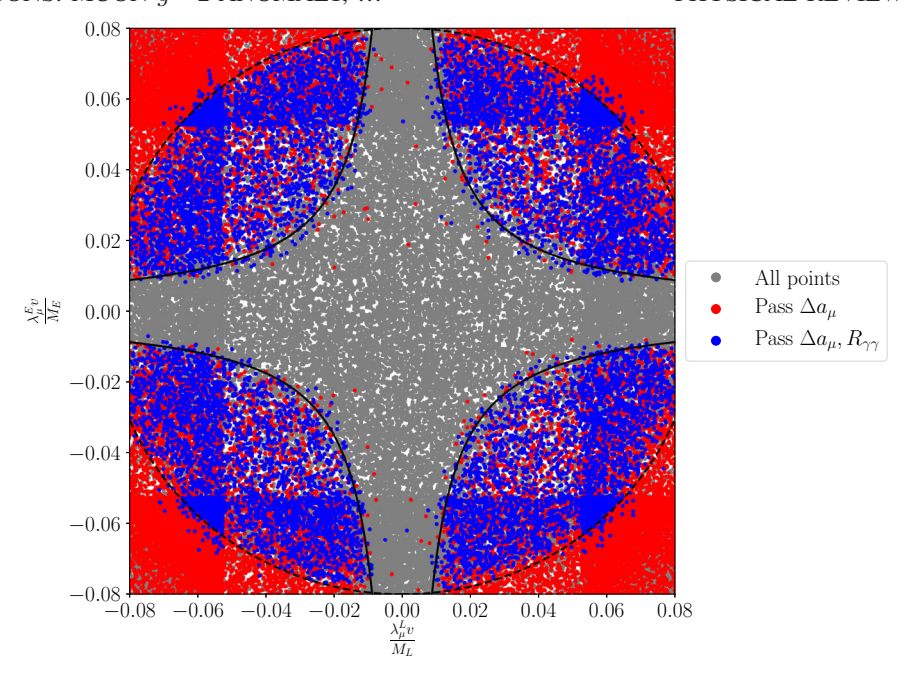


FIG. 6. Plot of the muon-VL couplings,  $\lambda_{\mu}^{E}v/M_{E}$  versus  $\lambda_{\mu}^{L}v/M_{L}$ . The solid and dashed black lines are the approximate empirical bounds on the muon-VL couplings. These bounds are not exact, but are obtained empirically (see text for more discussions).

the VL masses. From this figure, we see that this model requires  $\|\lambda_{\mu}\| > 0.03$  to fit  $\Delta a_{\mu}$  within  $1\sigma$  and  $\|\lambda_{\mu}\| < 0.09$  to fit  $R_{\gamma\gamma}$ .

Figure 6 shows a plot of  $\lambda_{\mu}^{L}$  versus  $\lambda_{\mu}^{E}$ . The gray points are all simulated points. The red points satisfy  $\Delta a_{\mu}$  within  $1\sigma$ , while the blue points are consistent with  $\Delta a_{\mu}$  and  $R_{\gamma\gamma}$ . To satisfy  $\Delta a_{\mu}$ , the muon-VL couplings need to satisfy approximately the following condition,

$$\left| \frac{\lambda_{\mu}^{E} v}{M_{E}} \frac{\lambda_{\mu}^{L} v}{M_{L}} \right| \gtrsim 7 \times 10^{-4},\tag{31}$$

which is shown by the solid lines. This bound is not an exact bound, but is an empirically obtained bound satisfied by most simulated points. On the other hand, to satisfy both  $\Delta a_{\mu}$  and  $R_{\gamma\gamma}$ , the muon-VL couplings need to satisfy approximately the following condition,

$$\left( \frac{\lambda_{\mu}^{E} v}{M_{E}} \right)^{2} + \frac{1}{1.08} \left( \frac{\lambda_{\mu}^{L} v}{M_{L}} \right)^{2} \lesssim 0.08^{2}, \tag{32}$$

which is showed by the dashed black lines. Similarly, this is not an exact bound.

Figure 7 shows a plot of  $\Delta a_{\mu}$  versus BR( $\mu \rightarrow e \gamma$ ), which gives the strongest LFV constraint. The points in this plot are separated into four colors based on ranges of the ratio of electron-VL to muon-VL couplings,

$$\left\langle \frac{\lambda_e}{\lambda_\mu} \right\rangle \equiv \frac{1}{2} \left( \frac{\lambda_e^L}{\lambda_\mu^L} + \frac{\lambda_e^E}{\lambda_\mu^E} \right). \tag{33}$$

The dashed lines show the  $1\sigma$  and  $2\sigma$  bounds of  $\Delta a_{\mu}$ , and the upper bound of BR( $\mu \to e\gamma$ ). The solid line shows the central value of  $\Delta a_{\mu}$ . This figure shows that simultaneously satisfying BR( $\mu \to e\gamma$ ) and  $\Delta a_{\mu}$  to within  $1\sigma$  require  $\langle \lambda_e/\lambda_{\mu} \rangle \lesssim 10^{-4}$ . This figure shows that this model requires some level of fine-tuning.

The most stringent constraints for the tau-VL coupling is from electroweak observables. The sampling range for tau-VL couplings,  $\lambda_{\tau}^{L.E}v/M_{L.E} \in (-0.09, 0.09)$ , is based on electroweak constraints. The next strongest constraint for the tau-VL coupling is BR( $\tau \to \mu \gamma$ ). This constraint, however, does not rule out any value of the tau-VL couplings within the sampling range. Finally, BR( $h \to \mu \tau$ ) does not constrain the parameter space at all. This is in agreement with a previous analysis by Falkowski *et al.*, which shows that the constraint from LFV Higgs decays is at least four orders of magnitude smaller than that from BR( $\ell \to \ell' \gamma$ ) [12].

As for the lepton nonuniversality measurements, the calculated values of  $R_K$  and  $R_{K^{*0}}$  do not deviate from the SM predictions because the Wilson coefficients contain the SM-VL mixing matrices squared, which are highly constrained by electroweak precision measurements. The ranges of Wilson coefficients in this model are

<sup>&</sup>lt;sup>5</sup>The square shape in Fig. 6 is unphysical and is due to our choice of sampling range.

<sup>&</sup>lt;sup>6</sup>Out of all simulated points, four points that violate this bound with the largest violation being  $\langle \lambda_e / \lambda_u \rangle = 2 \times 10^{-4}$ .

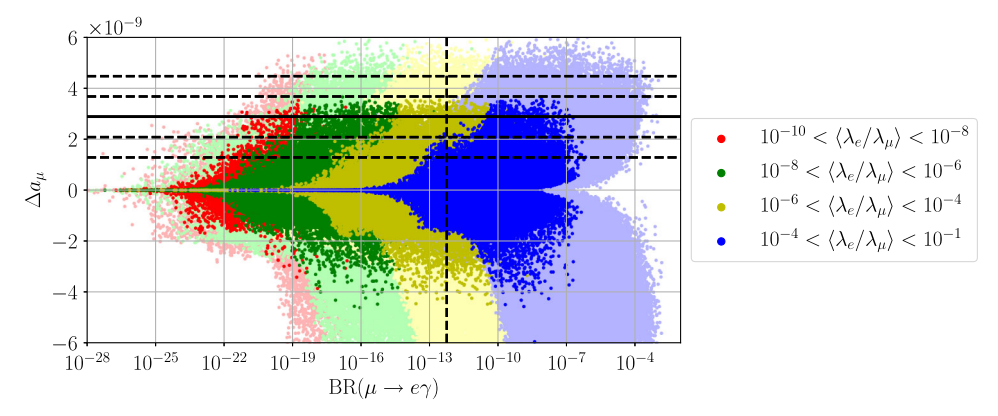


FIG. 7. Plot of  $\Delta a_{\mu}$  versus BR( $\mu \to e \gamma$ ), which gives the strongest LFV constraint. The lightly shaded points are ruled out. The dashed lines show the  $1\sigma$  and  $2\sigma$  bounds of  $\Delta a_{\mu}$ , and the upper bound of BR( $\mu \to e \gamma$ ). The solid line shows the central value of  $\Delta a_{\mu}$ . Simultaneously satisfying BR( $\mu \to e \gamma$ ) and  $\Delta a_{\mu}$  to within  $1\sigma$  requires  $\langle \lambda_e / \lambda_\mu \rangle \lesssim 10^{-4}$ .

$$\begin{split} -3.21 \times 10^{-11} &\leq C_9^{\text{NP}}(e) \leq 7.26 \times 10^{-12}, \\ -3.21 \times 10^{-11} &\leq C_{10}^{\text{NP}}(e) \leq 7.26 \times 10^{-12}, \\ -7.88 \times 10^{-3} &\leq C_9^{\text{NP}}(\mu) \leq 2.21 \times 10^{-3}, \\ -7.86 \times 10^{-3} &\leq C_{10}^{\text{NP}}(\mu) \leq 2.18 \times 10^{-3}. \end{split} \tag{34}$$

As a comparison, to fit all the *CP*-conserving  $b \to s \mu^+ \mu^-$  anomalies along with  $R_K$  and  $R_{K^{*0}}$ , the Wilson coefficients need to have values  $C_9^{\rm NP}(\mu) = -1.20 \pm 0.20$  and  $C_9^{\rm NP}(e) = C_{10}^{\rm NP}(e) = C_{10}^{\rm NP}(\mu) = 0$ , or  $C_9^{\rm NP}(\mu) = -C_{10}^{\rm NP}(\mu) = -0.68 \pm 0.12$  and  $C_9^{\rm NP}(e) = C_{10}^{\rm NP}(e) = 0$  [20].

## V. CONCLUSION

In this paper, we considered a very simple extension of the SM in which the SM is extended with one family of VL leptons; where the VL leptons couple to all three families of SM leptons. We studied the constraints on this model coming from the heavy charged lepton mass bound, electroweak precision data, the muon g-2, lepton flavor violation, Higgs decays and lepton nonuniversality observables. See Table II for the complete list of observables considered in this paper. All experimental values, other than lepton nonuniversality observables, are taken from the PDG [1]. The experimental value for  $R_K$  is taken from Ref. [10], while  $R_{K^{*0}}$  is recently measured by LHCb [11]. All theoretical calculations are performed at leading order, while the lepton nonuniversality observables are calculated using flavio [18].

In this paper, we showed that this model can fit all but the lepton nonuniversality measurements. The most constraining observables are the muon g-2,  $R_{\mu\mu}$ ,  $R_{\gamma\gamma}$  and the BR( $\mu \to e\gamma$ ). We find that if  $R_{\mu\mu}$  is measured to be SM-like, then this model cannot simultaneously fit both the muon g-2 within  $1\sigma$  and  $R_{\mu\mu}$  (see Fig. 2). In addition, we also find that the SU(2) doublet VL mass is required to satisfy  $M_L \lesssim 250$  GeV or  $M_L \gtrsim 400$  GeV in order to fit the muon g-2 within  $1\sigma$  (see Fig. 3). If the heavy charged lepton

mass bound increases to be above  $M_L \gtrsim 250$  GeV, then the muon g-2 can produce a stronger mass bound. Fitting to the muon g-2 requires  $||\lambda_{\mu}|| > 0.03$  while fitting to  $R_{\gamma\gamma}$ requires  $\|\lambda_{\mu}\| < 0.09$ . Hence, the muon-VL coupling is constrained to be within  $0.03 < ||\lambda_{\mu}|| < 0.09$ . Although we allow the VL leptons to couple to all three families of the SM leptons, by simultaneously fitting the muon g-2 and  $BR(\mu \to e\gamma)$ , the ratio of the electron-VL coupling to muon-VL coupling is constrained to be  $\langle \lambda_e / \lambda_\mu \rangle \lesssim 10^{-4}$ . Hence, this model requires some level of fine-tuning. On the other hand, the strongest constraints on the tau-VL coupling is coming from electroweak precision observables. The recently measured BR $(h \to \mu \tau)$  is less constraining than the electroweak precision observables. We also find that this model cannot explain the B physics lepton nonuniversality measurements.

#### ACKNOWLEDGMENTS

Z. P. and S. R. received partial support for this work from the DOE Grant No. DE-SC0011726. We would like to thank Andrzej Buras and Hong Zhang for discussions.

## APPENDIX A: BOX DIAGRAM CALCULATION

In this appendix, we calculate four box diagrams that have NP contributions to the decay of  $b \to s\ell\ell$ . As shown in Fig. 1, the NP contributions of these diagrams are due to VL leptons in the loop. The NP contribution enters via Wilson coefficients  $C_9$  and  $C_{10}$ . The calculation in the appendix is done in the 't Hooft-Feynman gauge.

# 1. Feynman rules

To see all the Feynman rules explicitly, we start by rewriting the Lagrangian that is relevant to our calculation. The definition of the fields and their corresponding quantum numbers are given in Table I. The Lagrangian of the leptonic sector is given in Eq. (3).

VECTORLIKE LEPTONS: MUON g-2 ANOMALY, ...

## a. W-lepton Couplings

From Eq. (13), we have

$$\mathcal{L} \supset \frac{g}{\sqrt{2}} [W_{\mu}^{+} \bar{\nu}_{a} \gamma^{\mu} ([\tilde{U}_{L}]_{ab} P_{L} + [\tilde{U}_{R}]_{ab} P_{R}) \hat{e}_{b}$$

$$+ W_{\mu}^{-} \bar{\hat{e}}_{b} \gamma^{\mu} ([\tilde{U}_{L}^{*}]_{ab} P_{L} + [\tilde{U}_{R}^{*}]_{ab} P_{R}) \nu_{a}], \tag{A1}$$

where  $P_{L,R}$  are projection operators and

$$\tilde{U}_L = \text{diag}(1, 1, 1, 1, 0)U_L$$
 (A2)

$$\tilde{U}_R = \text{diag}(0, 0, 0, 1, 0)U_R.$$
 (A3)

Notice that  $[U_L]_{4a} = [\tilde{U}_L]_{4a}$ , where a = 1, ..., 5. Similarly for  $U_R$ .

## b. Higgs-lepton couplings

Rewriting the Lagrangian, Eq. (3), in terms of the physical Higgs and the would-be Nambu-Goldstone bosons gives

$$\mathcal{L} \supset -\left(v + \frac{h}{\sqrt{2}}\right) \bar{e}_{L_{a}} Y_{ab}^{e} e_{R_{b}} - \frac{i\phi^{0}}{\sqrt{2}} \bar{e}_{L_{a}} Y_{ab}^{e\phi^{0}} e_{R_{b}} - \phi^{+} \bar{\nu}_{L_{b}} Y_{ba}^{\nu_{L}} e_{R_{a}} - \phi^{-} \bar{e}_{L_{a}} Y_{ab}^{\nu_{R}\dagger} \nu_{R_{b}} + \text{H.c.}.$$
(A4)

where  $Y^e$ ,  $Y^{\nu_L}$ , and  $Y^{\nu_R^{\dagger}}$  are given by Eq. (15), Eq. (23), and Eq. (24) respectively, and

$$Y^{e\phi^0} \equiv \begin{pmatrix} y_{ii}^e & 0 & \lambda_i^E \\ \lambda_i^L & 0 & \lambda \\ 0 & -\bar{\lambda} & 0 \end{pmatrix}. \tag{A5}$$

In the charged lepton mass basis, we have

$$\mathcal{L} \supset -\left(v + \frac{h}{\sqrt{2}}\right) \bar{\hat{e}}_{L_{a}} \hat{Y}_{ab}^{e} \hat{e}_{R_{b}} - \frac{i\phi^{0}}{\sqrt{2}} \bar{\hat{e}}_{L_{a}} [U_{L}^{\dagger} Y^{e\phi^{0}} U_{R}]_{ab} \hat{e}_{R_{b}} - \phi^{+} \bar{\nu}_{L_{b}} [Y^{\nu_{L}} U_{R}]_{ba} \hat{e}_{R_{a}} - \phi^{-} \bar{\hat{e}}_{L_{a}} [U_{L}^{\dagger} Y^{\nu_{R} \dagger}]_{ab} \nu_{R_{b}} + \text{H.c.}.$$
(A6)

So, the Feynman rules for the coupling in diagrams (b)–(d) in Fig. 1 involving the charged would-be Nambu-Goldstone bosons are

$$\phi^+$$
:  $-i([Y^{\nu_L}U_R]_{4a}P_R + [Y^{\nu_R}U_L]_{4a}P_L),$  (A7)

$$\phi^{-}:-i([Y^{\nu_L*}U_R^*]_{4a}P_L+[Y^{\nu_R*}U_L^*]_{4a}P_R).$$
 (A8)

Since all the calculations are performed in the charged lepton mass basis, to simplify notation, we will drop în the rest of this appendix.

## 2. Loop calculations

Before we start to evaluate the four diagrams in Fig. 1, let's consider two loop integrals that we will be using. These loop integrals are performed easily with Package-X developed by Patel [21].

$$A_{\alpha\beta}(M_i, M_L) \equiv \int \frac{d^4q}{(2\pi)^4} \frac{q_{\alpha}q_{\beta}}{(q^2 - M_W^2)^2 (q^2 - M_i^2)(q^2 - M_L^2)}$$
$$= -\frac{i}{64\pi^2 M_W^2} g_1(x_i, y) g_{\alpha\beta}, \tag{A9}$$

$$B(M_i, M_L) \equiv \int \frac{d^4q}{(2\pi)^4} \frac{1}{(q^2 - M_W^2)^2 (q^2 - M_i^2)(q^2 - M_L^2)}$$
$$= -\frac{i}{16\pi^2 M_W^4} g_0(x_i, y), \tag{A10}$$

where  $x_i = M_i^2 / M_W^2$ ,  $y = M_L^2 / M_W^2$  and

$$g_1(x,y) = \frac{1}{x-y} \left[ \frac{x^2}{(x-1)^2} \log x - \frac{y^2}{(y-1)^2} \log y - \frac{1}{x-1} + \frac{1}{y-1} \right],$$
 (A11)

$$g_0(x,y) = \frac{1}{x-y} \left[ \frac{x}{(x-1)^2} \log x - \frac{y}{(y-1)^2} \log y - \frac{1}{x-1} + \frac{1}{y-1} \right].$$
 (A12)

## a. Diagram (a)

$$\begin{split} \Box^{(a)} &= \left(\frac{g}{\sqrt{2}}\right)^4 \sum_{i=u,c,t} V_{ib} V_{is}^* \int \frac{d^4q}{(2\pi)^4} \left(\frac{-i}{q^2 - M_W^2}\right)^2 \left[\bar{s}\gamma^\mu P_L \frac{i(\not q + M_i)}{q^2 - M_i^2} \gamma^\nu P_L b\right] \\ &\times \left[\bar{e}_a([U_L^*]_{4a}\gamma_\nu P_L + [U_R^*]_{4a}\gamma_\nu P_R) \frac{i(\not q + M_L)}{q^2 - M_L^2} ([U_L]_{4a}\gamma_\mu P_L + [U_R]_{4a}\gamma_\mu P_R) e_a\right] \\ &= \frac{g^4}{4} \sum_{i=u,c,t} V_{ib} V_{is}^* \int \frac{d^4q}{(2\pi)^4} \frac{1}{(q^2 - M_W^2)^2 (q^2 - M_i^2) (q^2 - M_L^2)} \left[\bar{s}\gamma^\mu P_L (\not q + M_i)\gamma^\nu P_L b\right] \\ &\times \left[\bar{e}_a([U_L^*]_{4a}\gamma_\nu P_L + [U_R^*]_{4a}\gamma_\nu P_R) (\not q + M_L) ([U_L]_{4a}\gamma_\mu P_L + [U_R]_{4a}\gamma_\mu P_R) e_a\right]. \end{split}$$

The last two square brackets can be written as

$$q_{\alpha}q_{\beta}[\bar{s}\gamma^{\mu}\gamma^{\alpha}\gamma^{\nu}P_Lb][\bar{e}_a\gamma_{\nu}\gamma^{\beta}\gamma_{\mu}(|[U_L]_{4a}|^2P_L+|[U_R]_{4a}|^2P_R)e_a],$$

where we have dropped terms linear in q. Using Eq. (A9),

$$\Box^{(a)} = \frac{g^4}{4} \sum_{i=u.c.t} V_{ib} V_{is}^* A_{\alpha\beta}(M_i, M_L) [\bar{s} \gamma^{\mu} \gamma^{\alpha} \gamma^{\nu} P_L b] [\bar{e}_a \gamma_{\nu} \gamma^{\beta} \gamma_{\mu} (|[U_L]_{4a}|^2 P_L + |[U_R]_{4a}|^2 P_R) e_a].$$

Using  $g_{\alpha\beta}$  from  $A_{\alpha\beta}$ , the last two square brackets can be written as

$$[\bar{s}\gamma^{\mu}\gamma^{\alpha}\gamma^{\nu}P_Lb][\bar{e}_a\gamma_{\nu}\gamma_{\alpha}\gamma_{\mu}(|[U_L]_{4a}|^2P_L+|[U_R]_{4a}|^2P_R)e_a].$$

Using the following Dirac matrix identity,

$$\gamma^{\mu}\gamma^{\alpha}\gamma^{\nu} = g^{\mu\alpha}\gamma^{\nu} + g^{\alpha\nu}\gamma^{\mu} - g^{\mu\nu}\gamma^{\alpha} - i\epsilon^{\beta\mu\alpha\nu}\gamma_{\beta}\gamma^{5},$$

we can rewrite the last two square brackets as

$$4[\bar{s}\gamma^{\mu}P_{L}b][\bar{e}_{a}\gamma_{\mu}(|[U_{L}]_{4a}|^{2}P_{L}+|[U_{R}]_{4a}|^{2}P_{R})e_{a}].$$

Putting all these together, we have

$$\Box^{(a)} = -i \frac{4G_F}{\sqrt{2}} \sum_{i=u,c,t} V_{ib} V_{is}^* \frac{e^2}{16\pi^2} \frac{1}{s_W^2} \frac{1}{2} g_1(x_i, y) [\bar{s}\gamma^{\mu} P_L b] [\bar{e}_a \gamma_{\mu} (|[U_L]_{4a}|^2 P_L + |[U_R]_{4a}|^2 P_R) e_a].$$

Hence, the contributions of this diagram to the Wilson coefficients are

$$C_9^{\text{NP(a)}} = -\frac{1}{s_W^2} \frac{1}{4} (|[U_L]_{4a}|^2 + |[U_R]_{4a}|^2) g_1(x_i, y),$$

$$C_{10}^{\text{NP(a)}} = \frac{1}{s_W^2} \frac{1}{4} (|[U_L]_{4a}|^2 - |[U_R]_{4a}|^2) g_1(x_i, y). \tag{A13}$$

# b. Diagram (b)

$$\begin{split} \Box^{(b)} &= \left(\frac{g}{\sqrt{2}}\right)^4 \sum_{i=u,c,t} V_{ib} V_{is}^* \int \frac{d^4q}{(2\pi)^4} \left(\frac{-i}{q^2 - M_W^2}\right)^2 \left[\bar{s}\gamma^\mu P_L \frac{i(q+M_i)}{q^2 - M_i^2} \frac{M_i}{M_W} P_L b\right] \\ &\times \left[\bar{e}_a \frac{-v([Y^{\nu_L*}U_R^*]_{4a} P_L + [Y^{\nu_R*}U_L^*]_{4a} P_R)}{M_W} \frac{i(q+M_L)}{q^2 - M_L^2} ([U_L]_{4a} \gamma_\mu P_L + [U_R]_{4a} \gamma_\nu P_R) e_a\right] \\ &= \frac{g^4}{4} \sum_{i=u,c,t} V_{ib} V_{is}^* \int \frac{d^4q}{(2\pi)^4} \frac{1}{(q^2 - M_W^2)^2 (q^2 - M_i^2) (q^2 - M_L^2)} \left[\bar{s}\gamma^\mu P_L (q+M_i) \frac{M_i}{M_W} P_L b\right] \\ &\times \left[\bar{e}_a \frac{-v([Y^{\nu_L*}U_R^*]_{4a} P_L + [Y^{\nu_R*}U_L^*]_{4a} P_R)}{M_W} (q+M_L) ([U_L]_{4a} \gamma_\mu P_L + [U_R]_{4a} \gamma_\mu P_R) e_a\right]. \end{split}$$

The last two square brackets can be written as

$$-\frac{vM_i^2M_L}{M_{vv}^2}[\bar{s}\gamma^{\mu}P_Lb][\bar{e}_a\gamma_{\mu}([U_L]_{4a}[Y^{\nu_R*}U_L^*]_{4a}P_L+[U_R]_{4a}[Y^{\nu_L*}U_R^*]_{4a}P_R)e_a],$$

where we have dropped terms linear in q. Using Eq. (A10),

VECTORLIKE LEPTONS: MUON g-2 ANOMALY, ...

$$\Box^{(b)} = -\frac{g^4}{4} \sum_{i=u,c,t} V_{ib} V_{is}^* B(M_i,M_L) \frac{v M_i^2 M_L}{M_W^2} [\bar{s} \gamma^{\mu} P_L b] [\bar{e}_a \gamma_{\mu} ([U_L]_{4a} [Y^{\nu_R *} U_L^*]_{4a} P_L + [U_R]_{4a} [Y^{\nu_L *} U_R^*]_{4a} P_R) e_a].$$

Putting all these together, we have

$$\Box^{(b)} = i \frac{4G_F}{\sqrt{2}} \sum_{i=u,c,t} V_{ib} V_{is}^* \frac{e^2}{16\pi^2} \frac{1}{s_W^2} \frac{1}{2} \frac{v}{M_L} x_i y g_0(x_i, y) [\bar{s} \gamma^\mu P_L b] [\bar{e}_a \gamma_\mu ([U_L]_{4a} [Y^{\nu_R *} U_L^*]_{4a} P_L + [U_R]_{4a} [Y^{\nu_L *} U_R^*]_{4a} P_R) e_a].$$

Hence, the contributions of this diagram to the Wilson coefficients are

$$C_9^{\text{NP(b)}} = \frac{1}{s_W^2} \frac{1}{4} \frac{v}{M_L} x_i y([U_L]_{4a} [Y^{\nu_R *} U_L^*]_{4a} + [U_R]_{4a} [Y^{\nu_L *} U_R^*]_{4a}) g_0(x_i, y),$$

$$C_{10}^{\text{NP(b)}} = -\frac{1}{s_W^2} \frac{1}{4} \frac{v}{M_L} x_i y([U_L]_{4a} [Y^{\nu_R *} U_L^*]_{4a} - [U_R]_{4a} [Y^{\nu_L *} U_R^*]_{4a}) g_0(x_i, y). \tag{A14}$$

## c. Diagram (c)

$$\begin{split} \Box^{(c)} &= \left(\frac{g}{\sqrt{2}}\right)^4 \sum_{i=u,c,t} V_{ib} V_{is}^* \int \frac{d^4q}{(2\pi)^4} \left(\frac{-i}{p^2 - M_W^2}\right)^2 \left[\bar{s} \, \frac{M_i}{M_W} P_R \frac{i(\dot{q} + M_i)}{q^2 - M_i^2} \gamma^\mu P_L b\right] \\ &\times \left[\bar{e}_a([U_L^*]_{4a} \gamma_\mu P_L + [U_R^*]_{4a} \gamma_\mu P_R) \frac{i(\dot{q} + M_L)}{q^2 - M_L^2} \frac{-v([Y^{\nu_L} U_R]_{4a} P_R + [Y^{\nu_R} U_L]_{4a} P_L)}{M_W} e_a\right] \\ &= \frac{g^2}{4} \sum_{i=u,c,t} V_{ib} V_{is}^* \int \frac{d^4q}{(2\pi)^4} \frac{1}{(q^2 - M_W^2)^2 (q^2 - M_i^2) (q^2 - M_L^2)} \left[\bar{s} \, \frac{M_i}{M_W} P_R (\dot{q} + M_i) \gamma^\mu P_L b\right] \\ &\times \left[\bar{e}_a([U_L^*]_{4a} \gamma_\mu P_L + [U_R^*]_{4a} \gamma_\mu P_R) (\dot{q} + M_L) \frac{-v([Y^{\nu_L} U_R]_{4a} P_R + [Y^{\nu_R} U_L]_{4a} P_L)}{M_W} e_a\right]. \end{split}$$

The last two square brackets can be written as

$$-\frac{vM_{i}^{2}M_{L}}{M_{W}^{2}}[\bar{s}\gamma^{\mu}P_{L}b][\bar{e}_{a}\gamma_{\mu}([U_{L}^{*}]_{4a}[Y^{\nu_{R}}U_{L}]_{4a}P_{L}+[U_{R}^{*}]_{4a}[Y^{\nu_{L}}U_{R}]_{4a}P_{R})e_{a}],$$

where we have dropped terms linear in q. Using Eq. (A10),

$$\Box^{(c)} = -\frac{g^4}{4} \sum_{i=u,c,t} V_{ib} V_{is}^* B(M_i,M_L) \frac{v M_i^2 M_L}{M_W^2} [\bar{s} \gamma^{\mu} P_L b] [\bar{e}_a \gamma_{\mu} ([U_L^*]_{4a} [Y^{\nu_R} U_L]_{4a} P_L + [U_R^*]_{4a} [Y^{\nu_L} U_R]_{4a} P_R) e_a].$$

Putting all these together, we have

$$\Box^{(c)} = i \frac{4G_F}{\sqrt{2}} \sum_{i=u,c,t} V_{ib} V_{is}^* \frac{e^2}{16\pi^2} \frac{1}{s_W^2} \frac{1}{2} \frac{v}{M_L} x_i y g_0(x_i,y) [\bar{s} \gamma^\mu P_L b] [\bar{e}_a \gamma_\mu ([U_L^*]_{4a} [Y^{\nu_R} U_L]_{4a} P_L + [U_R^*]_{4a} [Y^{\nu_L} U_R]_{4a} P_R) e_a].$$

Hence, the contributions of this diagram to the Wilson coefficients are

$$C_9^{\text{NP(c)}} = \frac{1}{s_W^2} \frac{1}{4} \frac{v}{M_L} x_i y([U_L^*]_{4a} [Y^{\nu_R} U_L]_{4a} + [U_R^*]_{4a} [Y^{\nu_L} U_R]_{4a}) g_0(x_i, y),$$

$$C_{10}^{\text{NP(c)}} = -\frac{1}{s_W^2} \frac{1}{4} \frac{v}{M_L} x_i y([U_L^*]_{4a} [Y^{\nu_R} U_L]_{4a} - [U_R^*]_{4a} [Y^{\nu_L} U_R]_{4a}) g_0(x_i, y). \tag{A15}$$

## d. Diagram (d)

$$\begin{split} &\square^{(d)} = \left(\frac{g}{\sqrt{2}}\right)^4 \sum_{i=u,c,t} V_{ib} V_{is}^* \int \frac{d^4q}{(2\pi)^4} \left(\frac{-i}{q^2 - M_W^2}\right)^2 \left[\bar{s} \, \frac{M_i}{M_W} P_R \frac{i(\dot{q} + M_i)}{q^2 - M_i^2} \frac{M_i}{M_W} P_L b\right] \\ & \times \left[\bar{e}_a \frac{v([Y^{\nu_L*}U_R^*]_{4a} P_L + [Y^{\nu_R*}U_L^*]_{4a} P_R)}{M_W} \frac{i(\dot{q} + M_L)}{q^2 - M_L^2} \frac{v([Y^{\nu_L}U_R]_{4a} P_R + [Y^{\nu_R}U_L]_{4a} P_L)}{M_W} e_a\right] \\ & = \frac{g^4}{4} \sum_{i=u,c,t} V_{ib} V_{is}^* \int \frac{d^4q}{(2\pi)^4} \frac{1}{(q^2 - M_W^2)(q^2 - M_i^2)(q^2 - M_L^2)} \left[\bar{s} \, \frac{M_i}{M_W} P_R (\dot{q} + M_i) \frac{M_i}{M_W} P_L b\right] \\ & \times \left[\bar{e}_a \, \frac{v([Y^{\nu_L*}U_R^*]_{4a} P_L + [Y^{\nu_R*}U_L^*]_{4a} P_R)}{M_W} (\dot{q} + M_L) \frac{v([Y^{\nu_L}U_R]_{4a} P_R + [Y^{\nu_R}U_L]_{4a} P_L)}{M_W} e_a\right]. \end{split}$$

The last two square brackets can be written as

$$q_{\alpha}q_{\beta}\frac{v^{2}M_{i}^{2}}{M_{W}^{4}}[\bar{s}\gamma^{\alpha}P_{L}b][\bar{e}_{a}\gamma^{\beta}(|[Y^{\nu_{R}}U_{L}]_{4a}|^{2}P_{L}+|[Y^{\nu_{L}}U_{R}]_{4a}|^{2}P_{R})e_{a}],$$

where we have dropped terms linear in q. Using Eq. (A9),

$$\Box^{(d)} = \frac{g^4}{4} \sum_{i=u.c.t} V_{ib} V_{is}^* A_{\alpha\beta}(M_i, M_L) \frac{v^2 M_i^2}{M_W^4} [\bar{s} \gamma^{\alpha} P_L b] [\bar{e}_a \gamma^{\beta} (|[Y^{\nu_R} U_L]_{4a}|^2 P_L + |[Y^{\nu_L} U_R]_{4a}|^2 P_R) e_a].$$

Putting all these together, we have

$$\Box^{(d)} = -i \frac{4G_F}{\sqrt{2}} \sum_{i=u,c,l} V_{ib} V_{is}^* \frac{e^2}{16\pi^2} \frac{1}{s_W^2} \frac{1}{8} \frac{v^2}{M_L^2} x_i y g_1(x_i, y) [\bar{s} \gamma^{\mu} P_L b] [\bar{e}_a \gamma_{\mu} (|[Y^{\nu_R} U_L]_{4a}|^2 P_L + |[Y^{\nu_L} U_R]_{4a}|^2 P_R) e_a].$$

Hence, the contributions of this diagram to the Wilson coefficients are

$$C_9^{\text{NP(d)}} = -\frac{1}{s_W^2} \frac{1}{16} \frac{v^2}{M_L^2} x_i y(|[Y^{\nu_R} U_L]_{4a}|^2 + |[Y^{\nu_L} U_R]_{4a}|^2) g_1(x_i, y),$$

$$C_{10}^{\text{NP(d)}} = \frac{1}{s_W^2} \frac{1}{16} \frac{v^2}{M_L^2} x_i y(|[Y^{\nu_R} U_L]_{4a}|^2 - |[Y^{\nu_L} U_R]_{4a}|^2) g_1(x_i, y). \tag{A16}$$

## e. Total contributions

The sum of the Wilson coefficients from these four diagrams (Eq. (A13)–Eq. (A16)) is the total NP Wilson coefficients,

$$C_9^{\text{NP}} = -\frac{1}{s_W^2} \frac{1}{4} [U_1^+(x, y)g_1(x, y) + U_0^+(x, y)g_0(x, y)],$$

$$C_{10}^{\text{NP}} = \frac{1}{s_W^2} \frac{1}{4} [U_1^-(x, y)g_1(x, y) + U_0^-(x, y)g_0(x, y)],$$
(A17)

where  $x = M_t^2 / M_W^2$ ,  $y = M_L^2 / M_W^2$ ,

$$g_1(x,y) = \frac{1}{x-y} \left[ \frac{x^2}{(x-1)^2} \log x - \frac{y^2}{(y-1)^2} \log y - \frac{1}{x-1} + \frac{1}{y-1} \right],\tag{A18}$$

$$g_0(x,y) = \frac{1}{x-y} \left[ \frac{x}{(x-1)^2} \log x - \frac{y}{(y-1)^2} \log y - \frac{1}{x-1} + \frac{1}{y-1} \right], \tag{A19}$$

VECTORLIKE LEPTONS: MUON g-2 ANOMALY, ...

and

$$U_1^{\pm}(x,y) = |[U_L]_{4a}|^2 \pm |[U_R]_{4a}|^2 + \frac{1}{4} \frac{v^2}{M_I^2} xy(|[Y^{\nu_R}U_L]_{4a}|^2 \pm |[Y^{\nu_L}U_R]_{4a}|^2), \tag{A20}$$

$$U_0^{\pm}(x,y) = -\frac{v}{M_L} xy([U_L]_{4a} [Y^{\nu_R*}U_L^*]_{4a} + [U_L^*]_{4a} [Y^{\nu_R}U_L]_{4a} \pm [U_R]_{4a} [Y^{\nu_L*}U_R^*]_{4a} \pm [U_R^*]_{4a} [Y^{\nu_L}U_R]_{4a}).$$
(A21)

- C. Patrignani *et al.* (Particle Data Group Collaboration), Review of particle physics, Chin. Phys. C 40, 100001 (2016).
- [2] R. Dermíšek and A. Raval, Explanation of the muon g-2 anomaly with vectorlike leptons and its implications for Higgs decays, Phys. Rev. D **88**, 013017 (2013).
- [3] F. del Aguila, J. de Blas, and M. Perez-Victoria, Effects of new leptons in electroweak precision data, Phys. Rev. D 78, 013010 (2008).
- [4] A. Joglekar, P. Schwaller, and C. E. M. Wagner, Dark matter and enhanced Higgs to di-photon rate from vectorlike leptons, J. High Energy Phys. 12 (2012) 064.
- [5] J. Kearney, A. Pierce, and N. Weiner, Vectorlike fermions and Higgs couplings, Phys. Rev. D 86, 113005 (2012).
- [6] K. Ishiwata and M. B. Wise, Phenomenology of heavy vectorlike leptons, Phys. Rev. D 88, 055009 (2013).
- [7] A. J. Buras and M. Munz, Effective Hamiltonian for  $B \rightarrow X_s e^+ e^-$  beyond leading logarithms in the NDR and HV schemes, Phys. Rev. D **52**, 186 (1995).
- [8] C. Bobeth, M. Misiak, and J. Urban, Photonic penguins at two loops and  $m_t$  dependence of BR[ $B \to X_s l^+ l^-$ ], Nucl. Phys. **B574**, 291 (2000).
- [9] T. Inami and C. S. Lim, Effects of superheavy quarks and leptons in low-energy weak processes  $k_L \to \mu \bar{\mu}$ ,  $K^+ \to \pi^+ \nu \bar{\nu}$  and  $K^0 \leftrightarrow \bar{K}^0$ , Prog. Theor. Phys. **65**, 297 (1981); Erratum, Prog. Theor. Phys. **65**, 1772(E) (1981).
- [10] R. Aaij *et al.* (LHCb Collaboration), Test of Lepton Universality using  $B^+ \to K^+ \ell^+ \ell^-$  Decays, Phys. Rev. Lett. **113**, 151601 (2014).

- [11] R. Aaij *et al.* (LHCb Collaboration), Test of lepton universality with  $B^0 \to K^{*0} \ell^+ \ell^-$  decays, arXiv:1705.05802.
- [12] A. Falkowski, D. M. Straub, and A. Vicente, Vector-like leptons: Higgs decays and collider phenomenology, J. High Energy Phys. 05 (2014) 092.
- [13] S. A. R. Ellis, R. M. Godbole, S. Gopalakrishna, and J. D. Wells, Survey of vectorlike fermion extensions of the standard model and their phenomenological implications, J. High Energy Phys. 09 (2014) 130.
- [14] R. Dermisek, J. P. Hall, E. Lunghi, and S. Shin, Limits on vectorlike leptons from searches for anomalous production of multi-lepton events, J. High Energy Phys. 12 (2014) 013.
- [15] N. Kumar and S. P. Martin, Vectorlike leptons at the large hadron collider, Phys. Rev. D 92, 115018 (2015).
- [16] L. Lavoura, General formulae for  $f_1 \rightarrow f_2 \gamma$ , Eur. Phys. J. C **29**, 191 (2003).
- [17] A. Djouadi, The Anatomy of electro-weak symmetry breaking. I: The Higgs boson in the standard model, Phys. Rep. 457, 1 (2008).
- [18] D. Straub, P. Stangl, C. Niehoff, E. Gurler, J. Kumar, sreicher, and F. Beaujean, flav-io/flavio v0.21.1, 2017.
- [19] A. Chapelain (Muong-2 Collaboration), The Muon g-2 experiment at Fermilab, EPJ Web Conf. 137, 08001 (2017).
- [20] A. K. Alok, B. Bhattacharya, A. Datta, D. Kumar, J. Kumar, and D. London, New physics in  $b \to s\mu^+\mu^-$  after the measurement of  $R_{K^*}$ , arXiv:1704.07397.
- [21] H. H. Patel, Package-X: A Mathematica package for the analytic calculation of one-loop integrals, Comput. Phys. Commun. **197**, 276 (2015).